Limnol. Oceanogr., 31(2), 1986, 305–318

Reconciling measured and predicted fluxes of oxygen across the deep sea sediment–water interface[1]

Clare E. Reimers and K. L. Smith, Jr.
Scripps Institution of Oceanography, University of California, San Diego, La Jolla 92093

Abstract

Rates of sediment community oxygen consumption determined in situ are compared to fluxes predicted from oxygen microelectrode gradients measured in cores from ~3,750-m water depth in the eastern North Pacific. Oxygen concentrations decrease exponentially over >1.5 cm and suggest that organic matter in the sediments is degraded most rapidly immediately below the sediment–water interface.

Molecular diffusion of oxygen across the interface is modeled as an "internal regime" and can account for nearly all the directly measured in situ flux, 0.20±0.02 μmol cm^{-2} d^{-1}. This differs from published accounts of nearshore marine environments, where activity of bottom-dwelling macrofauna or bubble ebullition enhances benthic fluxes of dissolved nutrients or gases 2–4 times. Millimeter depth-scale profiles of porosity, organic C, carbonate C, and bacterial abundance are reported to provide additional constraints on interface processes, including the relative effects of organic matter degradation and bioturbation. The highest organic C, bacterial, and porosity values are in the uppermost sediments (0–0.2 cm). Within the stratum 0–1 cm, porewater flux ratios of oxygen to nitrate support a model of exchange by diffusion leading to organic matter oxidation and nitrification according to Redfield stoichiometry. Below the oxygen reduction zone, changes in the porewater concentrations of NO_3^-, Mn^{2+}, Fe^{2+}, NH_4^+, and alkalinity indicate that anaerobic respiration reactions using NO_3^-, MnO_2, Fe_2O_3, and SO_4^{2-} as electron acceptors complete the early oxidation of organic matter at this site.

Fluxes of oxygen across sediment–seawater boundaries can serve as sensitive measurements for predicting rates of benthic organic matter oxidation. In deep sea environments, oxygen fluxes have been determined directly with in situ chambers (e.g. Smith 1978; Smith et al. 1978, 1979; Hinga et al. 1979) and indirectly with porewater profiles and Fick's law of diffusion (Murray and Grundmanis 1980; Goloway and Bender 1982; Jahnke et al. 1982; Reimers et al. 1984). Both techniques have been compared at a common location for determinations of the sediment–water exchange of methane, radon, ammonium, phosphate, CO_2, manganese, and silicate (McCaffrey et al. 1980; Klump and Martens 1981; Jahnke et al. 1983; Andrews and Hargrave 1984), but not for the exchange of oxygen.

When measured and predicted fluxes of exchangeable porewater constituents have not agreed in previous studies, both biochemical and systemic causes have been suspected. For the case of rates of sea floor oxygen utilization, biological or chemical processes which consume oxygen in tubes, burrows, or a very thin surface layer could lead to an excess flux that is not gradient supported. Likewise, if sampling methods disturb the natural system, or assumptions made in flux determinations are incorrect, measured or predicted fluxes may be systematically in error. Our major objective here was to compare in situ measurements of oxygen fluxes with predicted fluxes derived from detailed microelectrode oxygen gradients in the top centimeter of sediments from a deep Pacific Ocean site. The site chosen was in an abyssal plain region at the base of the Patton Escarpment.

We thank W. Stockton, D. Wahlberg, M. Laver, N. Brown, J. Edelman, and R. Wilson for assistance at sea with samples and equipment. A. A. Yayanos and J. Gieskes were generous with laboratory space and equipment, and T. Shaw provided advice on techniques for porewater analyses. Reviews of the manuscript were made by R. Jahnke, F. Sayles, D. Craven, S. Emerson, and W. Wakefield.

Materials and methods

In situ flux measurements, sediment and water samples—The Patton Escarpment site

[1] Support for this research was provided by NSF grants OCE 81-17661 and OCE 83-15306.

Table 1. Patton Escarpment samples.

Sta.	Recovery date (1984)	Sampler	N lat, W long	Water depth (m)	Sample status*
110-C	31 Mar	FVGR	32°32.4′, 120°36.8′	3,779	3, 4, 5
124-C	5 Apr	FVGR	32°29.9′, 120°38.5′	3,730	1, 2, 4, 7
128-C	5 Apr	Soutar box core	32°32.4′, 120°39.0′	3,738	2, 3, 4, 5, 6

* Data available: 1—O_2 consumption rate by FVGR; 2—porewater constituents; 3—fine-scale porosity; 4—organic carbon and carbonate carbon; 5—O_2 microelectrode; 6—bacteria numbers; 7—macrofauna numbers and biomass.

has been studied by one of us (K.L.S.) over the past 7 years and exhibits a seasonal pattern of sediment community oxygen consumption that varies by as much as a factor of four and is probably related to the productivity of overlying waters (Smith and Baldwin 1984). As before, we used a free vehicle grab respirometer (FVGR) to determine oxygen uptake and nitrogenous nutrient exchange across the sediment–water interface and nutrient profiles above and below the interface (Smith et al. 1983; Smith and Baldwin 1983). The instrument package of the FVGR is composed of four 20- × 20-cm replicate grab/respiration chambers, each of which has an associated oxygen sensor to measure the uptake during incubation, a stirring motor to prevent stratification inside the chambers, and two 50-ml syringes to withdraw filtered water samples (0.4-μm Nuclepore filters) for determination of nutrient concentrations at the beginning and end of the incubation. The incubation period was 67 h from 2 to 5 April 1984 (Sta. 124-C). Sediment cores (9-cm diam) for porewater and organic and carbonate carbon analyses from two grabs were taken to a refrigerated van (2°C±2°) within an hour after the FVGR was recovered. The cores had intact surfaces, clear overlying water, and were about 10 cm long. Sediments from the other two grabs were put through a 297-μm sieve for analyses of macrofaunal abundance and wet weight biomass.

A 30- × 30-cm Soutar box core collected during the same sampling period had an intact sediment–water interface with slightly turbid overlying water and was processed for microelectrode oxygen, porewater constituents, fine-scale porosity profiles, organic and carbonate carbon, and bacterial numbers by epifluorescent counts. Table 1 summarizes the locations and data from the spring sampling period. Station 110-C was an unsuccessful FVGR deployment because the grab exchange ports did not close, but it is included to illustrate the effects of surface water exchange and physical disturbance on porewater gradients.

Microelectrode oxygen gradients—The microelectrode oxygen measurements were made in the refrigerated van, in sediment that had been subcored from each sampler with a butyrate core liner and then tightly capped without any airspace. The experimental set-up and procedures were as described by Reimers et al. (1984). The water layer over the cores (5–8 cm) was not stirred during the measurements to avoid increasing the aeration that occurs because bottom waters are undersaturated with respect to atmospheric P_{O_2}. Immediately after recovery, the water overlying the sediments collected in the Soutar box core was 8°C and had an oxygen concentration of 138.4±1.2 μmol kg^{-1}, very close to a near-bottom value of 135.9 (B.W. temp = 1.5°C) determined from water collected about 10 m above the seafloor in a CTD/rosette Niskin bottle. The overlying water in the sample from the unsuccessful FVGR (Sta. 110-C) was 14°C and had an oxygen concentration of 225±4 μmol kg^{-1} upon recovery. Profiles from both the Soutar box core and the first FVGR deployment were measured <2.5 h after the samples came on deck. Oxygen profiles were not measured in the grab samples from the second FVGR deployment (Sta. 124-C) because storm conditions prevented work with the microelectrodes.

Bacterial counts, porosity, and organic carbon—Sediment samples for fine-scale profiles of bacterial concentrations, poros-

ity, and organic carbon content were collected by inserting beveled 50-ml plastic syringes (3-cm diam) into the top 4–6 cm of the grab or box cores and then sectioning the syringe samples in the cold van at 1–10-mm intervals. Because of temperature constraints (>10°C kills deep sea bacteria: Yayanos and Dietz 1982), only one such syringe was collected for bacterial counts (Table 1). Subsamples (1 cm^3) were fixed in acid-cleaned, UV-radiated, glass scintillation vials containing 10 ml of a 0.2-μm-filtered seawater solution of 4% formaldehyde. These samples were stored at 2°C until they could be processed on shore (6 weeks).

Processing methods for the bacterial subsamples were similar to the procedures of DeFlaun and Mayer (1983). For direct counting, each fixed sample was placed on a vortex mixer, and 1.0 ml of homogenized sample was pipetted into a 10-ml centrifuge tube containing 0.1 ml of the fluorescent stain DAPI (4′-6-diamiamidino-2-phenylindole dihydrochloride; 0.5 $\mu g\ ml^{-1}$). These tubes were also vortexed and stored in a dark refrigerator overnight. Slides were prepared by diluting 0.050 ml of stained sample in 4 ml of a solution of artificial seawater, 0.25% formaldehyde, and 0.05% sodium azide, and then filtering the entire volume through a 0.2-μm Iragalan black-stained Nuclepore filter (25-mm diam). The filter was mounted on a glass slide in paraffin oil and examined under a Zeiss Universal microscope with an HBO-100 Hg illuminator source and UV filter set No. 487702. Fifty fields (0.0061 mm^2) were counted for each slide, and the mean number of particles <2 μm that fluoresced bright blue per field were used to calculate the total number of bacteria per milliliter of wet sediment (Porter and Feig 1980). Blue fluorescent particles >2 μm were also counted as a measure of the vertical distribution of nanobiota.

Separate syringe samples of sediment were sectioned at sea for the porosity and organic carbon analyses, frozen, and later freeze-dried in the laboratory. Porosity was determined from dry weight and chlorinity measurements by wetting a known weight of dry sample (~0.1 g) with 1 ml of distilled water and titrating, in duplicate, 0.10 ml of supernatant with 0.1 N $AgNO_3$ and a potassium dichromate-chromate indicator. The precision of the chlorinity titration is 1% or better, and porosity is calculated assuming a dry bulk density of 2.5 g cm^{-3} and a porewater salinity of 35‰.

Carbon analyses were made in duplicate with a Coulometrics carbon analyzer and corrected to a salt-free basis with the porosity data. The Coulometrics carbon analyzer measures carbonate carbon and total carbon separately after carbon dioxide is liberated from sample splits by acidifying (carbonate C) or heating at 950°C (total C). The liberated CO_2 is swept through a scrubber by a CO_2-free carrier gas into an absorption cell where it is converted to a strong acid and then coulometrically titrated. Organic carbon is calculated as the difference between total and carbonate carbon. The average precision of both the duplicate total and carbonate measurements was ±0.01% C, but the porosity correction increases the uncertainty to ±0.02% C.

Porewater analyses—Porewater cores were sectioned at 1–2-cm intervals at 2°C±2° and the outer layer (~0.5 cm) was removed to eliminate possible effects of streaming. The porewater was extracted by centrifugation (16,000 rpm, 2°C, 5 min) and filtered through 0.4-μm Nuclepore filters. Ammonium and silicate analyses were run at sea; other analyses were made 3–4 weeks later on shore on acidified (NO_3^-, NO_2^-, Mn^{2+}, Fe^{2+}) or nonacidified (alkalinity) samples. The acid used was redistilled 6 N HCl, and the porewaters were stored refrigerated in acid-cleaned polyethylene vials. Although two 9-cm-diam subcores were processed separately from the FVGR grabs and the Soutar box core, a few of the sampled intervals did not yield enough porewater for all analyses; in these cases one analysis (usually ammonium) had to be omitted.

The procedures used for the porewater chemistry and the precisions derived as mean standard deviations of duplicate measurements were:

Alkalinity—the Gran titration as described by Gieskes and Rogers (1973) on 4-ml samples; $P = \pm 0.005$ meq kg^{-1};

Ammonium—the method of Strick-

Table 2. Measured fluxes, μmol cm^{-2} d^{-1}. Negative fluxes are into the sediment; positive fluxes are out of the sediment.

Oxygen (n = 3)	Nitrate + nitrite (n = 3)	Ammonium (n = 2)
−0.18 to −0.22	−0.00083 to +0.0067	+0.00032 to +0.00096

land and Parsons (1972) adapted to 5-ml samples with absorbances read in a 10-cm cell; $P = \pm 0.5$ μmol kg^{-1};

Silicate—the molybdenum blue method of Mullin and Riley (1955) modified to 0.5-ml samples; $P = \pm 2$ μmol kg^{-1};

Manganese and iron—direct injection into a graphite furnace-atomic absorption analyzer (Froelich et al. 1979); $P \sim \pm 0.1$ μmol kg^{-1};

Nitrate and nitrite—the standard colorimetric method in which nitrite is determined directly and then subtracted from a "total" N determined after reducing nitrate to nitrite on a Cd column. For total N, 2-ml samples were readjusted to neutral pH and then diluted with 8 ml of distilled water before reduction. Nitrite was determined after reaction with sulfanilamide in acid solution, and *N*-(1-naphthyl)-ethylene diamine (Strickland and Parsons 1972). The resulting pink azo dye was measured with a Gilford spectrophotometer using a 1-cm cell. Although there were few replicates, we estimate $P \sim \pm 0.2$ μmol kg^{-1}.

Concentrations of all constituents were determined on a per volume basis and converted to a per mass basis by division by 1.024 kg liter^{-1}, the density of 35‰ seawater at 22°C.

Bottom water vs. overlying water analyses—The water overlying a core recovered on shipboard is seldom equivalent to true bottom water, due either to exchange between the cored sample and the water column during retrieval and recovery or to exchange with interstitial waters during the entire sampling period. For this reason overlying water samples in our cores were treated as "porewater" samples and are reported as the values at zero depth (*see Fig. 3*). Bottom water values of oxygen and nutrients which will be used in flux calculations and stoichiometric comparisons were determined from CTD cast samples (O_2) taken 10 m above the bottom and the initial FVGR syringe samples ($NO_3^- + NO_2^-$) taken within 10 cm of the bottom. These analyses were made onboard ship (Smith et al. 1983).

Results and discussion

Measured fluxes and downcore data—In situ rates of oxygen flux to and nitrogenous nutrient exchange across the Patton Escarpment sediments determined from the FVGR grabs (n = 3) at Sta. 124-C are reported in Table 2. The oxygen fluxes are intermediate between earlier replicate measurements at this site and consistent with the seasonal pattern (Smith and Baldwin 1984). Nitrogenous nutrient exchange rates are smaller and more variable than previous determinations at the site (Smith et al. 1983).

Subsurface profiles of microelectrode oxygen, sediment parameters, and porewater constituents in cores collected nearly simultaneously within a 6-km^2 area are shown in Figs. 1, 2, and 3. Because these profiles are very similar in the first 1–2 cm where oxygen had penetrated, we assume oxygen fluxes predicted from one set of downcore data represent the entire area. We evaluate these data below in terms of the parameters used to predict integrated rates of benthic oxygen consumption and in terms of oxidation reactions which consume organic carbon after it is buried beneath the seawater–sediment boundary. We are especially concerned with assessing which features are real and not artifacts caused by sampling or analytical techniques.

Parameters for calculating an oxygen flux—In shallow water marine environments, fluxes of seawater constituents across the sediment–water interface have been represented as the sum of a molecular diffusive term and a biogenic advective or quasi-dif-

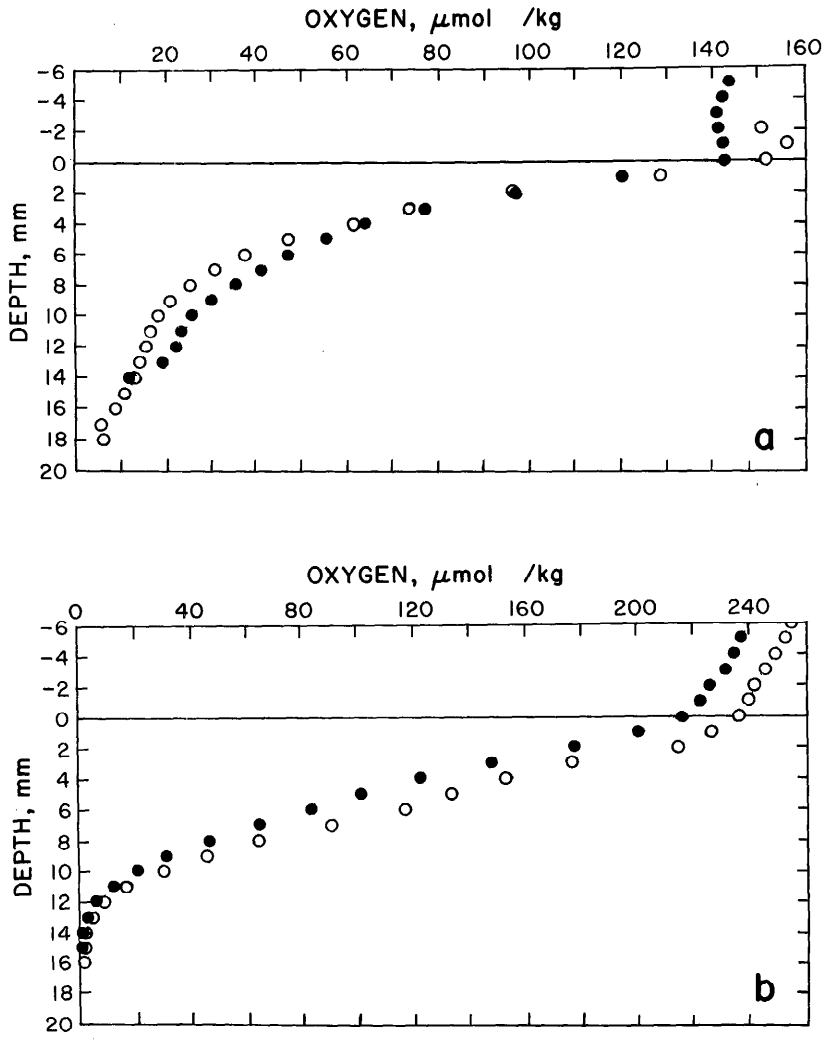

Fig. 1. Microelectrode oxygen gradients from the Patton Escarpment Soutar box core (a) and FVGR Sta. 110 core (b). The symbols designate two separate profile determinations (closed circles preceding open circles in time). The 0-cm depth horizon marks the sediment–water interface; however, overlying water concentrations are elevated above the bottom water concentration of 135.9 μmol kg^{-1}.

fusive term which can result from infaunal irrigation (McCaffrey et al. 1980), infaunal irrigation and the effects of burrows on diffusion geometry (Aller 1978, 1980), bubble ebullition (Martens and Klump 1980), or undetected interface reactions (Klump and Martens 1981). However, because the numbers and activity of bottom-dwelling organisms diminish with increasing water depth, molecular diffusion across a uniform planar surface has been assumed by many workers to be effectively the sole process controlling the benthic flux rates at deep ocean sites (e.g. Sayles 1979; Murray and Grundmanis 1980; Sawlan and Murray 1983). If we make this assumption also, then the oxygen consumption rate at the Patton Escarpment site can be calculated from three parameters which make up Fick's first law of diffusion as it is applied to sediments (Berner 1980). This flux equation is

$$F = -\phi_o D_s \left(\frac{dC}{dz}\right)_{z=0},$$

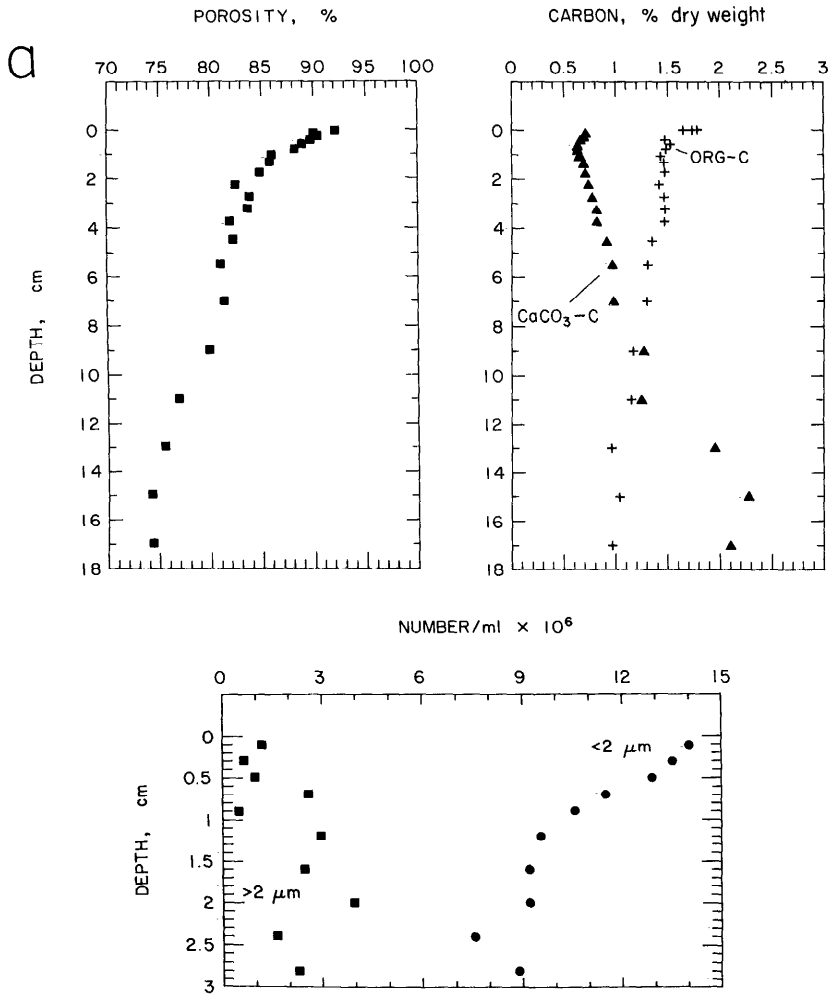

Fig. 2. Fine-scale profiles of porosity, organic C, carbonate C, and epifluorescent particle numbers in sediments from the Patton Escarpment (a—box core; b—FVGR Sta. 110; c—FVGR Sta. 124).

and the three parameters are $(dC/dz)_{z=0}$, the concentration gradient, in this case of oxygen, at the sediment–water interface (μmol cm^{-3} cm^{-1}), ϕ_o, the porosity at the interface (cm^3_{pw} $cm^{-3}_{bulk\ sed.}$), and D_s, the bulk sediment diffusion coefficient, also at the interface (cm^2 d^{-1}).

In Fig. 1, the two sets of microelectrode profiles from the subcores are plotted vs. depth. Of the two sets, the gradients for the Souter box core (Fig. 1a) are the least altered from in situ oxygen tensions and so best suited for estimating the first flux parameter, the oxygen gradient *at* the sediment–water interface. These data indicate that a typical value for the $z = 0$ oxygen gradient in the vicinity of the box core station fell within the range of 0.19–0.21 μmol cm^{-3} cm^{-1} during April 1984. We make this estimate by assuming that the oxygen concentrations in Fig. 1a are equal to in situ values at 0.2 cm and below in the sediments. Above the 0.2-cm level, handling had elevated the oxygen concentration, so the true in situ oxygen profiles are assumed to increase to a bottom water value of 135.9 μmol kg^{-1} at the sediment–water interface. That is, we imagine that on the seafloor, boundary layer gradients are very small and the oxygen flux is determined by the internal

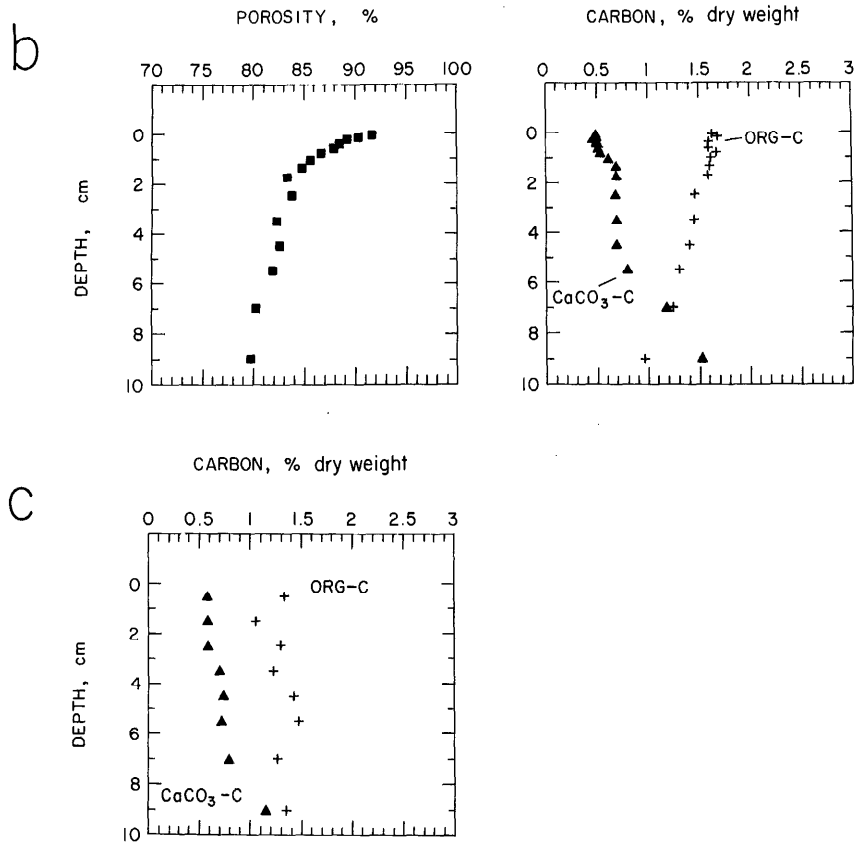

Fig. 2. Continued.

resistance to oxygen diffusion (Boudreau and Guinasso 1982). The gradient range of 0.19–0.21 μmol cm^{-3} cm^{-1} is calculated by considering all possible linear gradients between 0 cm and 0.2 or 0.3 cm (Fig. 1a). If linear extrapolations are made to the data points at 0.5 cm, the range of values for the predicted slope increases to 0.16–0.21 μmol cm^{-3} cm^{-1}. This comparison illustrates that interface gradient estimates generally decrease as the distance of extrapolation increases.

We justify our gradient assumptions and extrapolations to the 0.2- or 0.3-cm horizons because of certain observations. First, the two replicate profiles begin to exhibit convex curvature at $\leq$0.2 cm below the interface (depth = 0). Second, any inaccuracy in the near-interface concentrations illustrated in Fig. 1a due to calibration errors is not >10%. And finally, the oxygen concentration of the overlying water in the box core subcore had not greatly increased during the time the subcore was uncapped for the microelectrode measurements (*see* Reimers et al. 1984, for a mathematical model of contamination effects). In contrast, the oxygen profiles measured in the FVGR subcore from Sta. 110-C could not be used to estimate the $z = 0$ oxygen gradient. These gradients are obviously flattened and have highly elevated near-interface concentrations due to leakage of surface seawater into the grab. The oxygen zero boundary of the Sta. 110-C profiles was also encountered at a shallower depth (i.e. 1.5 cm) than in the box core sample. This is an indication that surface sediment may have been lost from this FVGR core (C. Reimers pers. obs.).

The second depth-dependent parameter

Table 3. Parameters used to predict an oxygen flux.

Depth (z) (cm)	Porosity (ϕ) ($cm^3\ cm^{-3}$)	Diffusion coef. (D_s) ($cm^2\ d^{-1}$)	O_2 gradient (dC/dz) ($\mu mol\ cm^{-3}\ cm^{-1}$)
0–0.3	0.89–1.0	0.85–1.07	0.19–0.21

that will be part of a flux calculation is porosity. The two fine-scale porosity profiles (Fig. 2a and b) reveal a nearly continuous decline from >92% at the sediment–water interface to <84% below 2-cm depth. Although in general both cores look similar and have reasonable porosities for surficial sediments with a high clay content (Berner 1980), careful cross-correlation of the porosity profiles supports our observation that we may not have sampled an intact sediment surface at Sta. 110-C. The same conclusion is more easily reached after comparing the fine-scale organic carbon and carbonate carbon profiles in Fig. 2a and b. From the carbon profiles, it appears that 1–2 cm of surface material was lost from the first FVGR core.

The remaining parameter needed for an oxygen flux prediction is the bulk sediment diffusion coefficient for oxygen at the sediment–water interface. Because the oxygen profiles in Fig. 1a extend into the sediment and show curvature from 0 to about 1.5 cm, reaction must occur over this interval, and the flux to this interval must be equal to the integrated reaction rate. This situation has been described by Boudreau and Guinasso (1982) as an "internal diffusion regime." It implies that if biological transport mechanisms are unimportant, then under in situ conditions, D_s must be less than or equal to the free solution diffusion coefficient (denoted D_o). The empirical relationship, $D_s = D_o \times \phi^2$, has been shown by Ullman and Aller (1982) to yield a close approximation for directly measured values of D_s for nonionic solutes in high porosity sediments. If D_s is constrained by this equation for $z \leq 0.3$ cm and $D_o = 1.07\ cm^2\ d^{-1}$ (Broecker and Peng 1974), then $\phi \geq 0.89$ and $0.85 \leq D_s \leq 1.07\ cm^2\ d^{-1}$. Table 3 summarizes the values of the three parameters that have been determined in order to predict the oxygen flux at the Patton Escarpment site.

Table 4. Abundance and biomass of macrofauna per grab (0.0412 m^2) at Sta. 124-C.

Taxa	Numbers		Wet weight (mg)	
	Grab B	Grab C	Grab B	Grab C
Polychaeta	67	67	19.0	12.7
Nematoda	74	65	2.9	1.2
Copepoda	12	13	—	—
Tanaidacea	2	2	·	·
Isopoda	3	5	·	·
Ostracoda	3	0	·	·
Bivalvia	2	3	1.7	2.7
Ophiuroidea	1	0	·	·
Amphipoda	1	0	·	·
Cumacea	2	0	·	·
Other	3	0	—	—
Avg No. organisms m^{-2}		3,945		
Avg biomass (mg m^{-2})		487.8		

Biomass and carbon distributions—We have implied above that rates of oxygen consumption and therefore respiratory reactions are greatest within the first few millimeters of the sediments from the Patton Escarpment site. If this pattern is not solely a function of the oxygen concentration, then the parameters most likely to affect the magnitudes of these rates are the availability of utilizable organic carbon and benthic biomass.

Both organic carbon and bacterial cell numbers <2 μm decrease in the first 1.5 cm of the box core sample (Fig. 2a). The vertical distribution of fluorescent particles >2 μm, which we interpret to represent nanobiota, has a more random pattern. Vertical distributions of metazoan organisms were not determined, but the abundance and wet weight biomass of benthic macrofauna per unit area for two grabs at Sta. 124-C are presented in Table 4. If we assume that all these organisms were situated within the first 1.5 cm of the sediment, where oxygen is most readily available, then on average they occupy ~0.003% of the total volume of that sediment layer and contribute $\sim 3 \times 10^{-7}$ g C per g sediment, or <0.001% of the organic carbon. (This assumes 1.02 g wet wt cm^{-3} biovolume: Snider et al. 1984, and 2×10^{-3} g C cm^{-3} biovolume.) In terms of volume or carbon, bacteria contribute about equally in magnitude (assuming 10^{-14} g C $cell^{-1}$: A. F. Carlucci pers. comm.), and meiofaunal

organisms are also probably comparable to the macrofaunal assemblage (Snider et al. 1984). These calculations rule out the possibility that the organic carbon profiles reflect the vertical distribution of organisms rather than the distribution of detrital organic matter.

The importance of the above conclusion is that it implies that surficial organic carbon gradients like that in Fig. 2a could mirror distributions of aerobic respiration rates or at least provide a measure of the relative rates of organic matter degradation and bioturbation at deep ocean sites. If bioturbation is a random but slow process relative to a first-order organic matter oxidation reaction, carbon profile curvatures will be steep (Emerson et al. 1985). For such a situation there should also be little effect of relict macrobenthos tubes or burrows on a total oxygen flux, because most of the oxygen consumption must occur very near the sediment–water interface where diffusion distances are very small (Aller 1980, 1984). At the Patton Escarpment, our steep near-surface box core carbon profiles suggest that bioturbation was insufficiently rapid to cause the most labile organic carbon to be mixed very far into the sediment before oxidation or that it was nonrandom. This case cannot be made for the FVGR cores (Fig. 2b and c), but as already discussed, we believe that surface material is missing from the core from Sta. 110-C and that the Sta. 124-C sediments were sampled over intervals too large to see such an effect.

The extended depth scale of organic matter oxidation—Although reaction rates decline below the near-interface zone, the compositions of porewaters in subsurface deep sea sediments continue to depend on diffusion, endemic organisms, and a sequence of oxidation-reduction reactions which are ordered by the free energy released during the oxidation of organic carbon (Froelich et al. 1979; Emerson et al. 1980). Oxygen reduction is the first and dominant reaction in this sequence (>90% of the rain rate of organic carbon is usually oxidized aerobically: Bender and Heggie 1984), but the porewater concentration gradients from the box core and the second, more successful, FVGR deployment (Sta. 124-C) demonstrate a few unexpected consequences of the entire reaction sequence.

From Fig. 3 it is evident that in the first 1–2 cm of the Patton Escarpment sediments oxygen must be rapidly depleted, producing nitrate and very small amounts of the reaction intermediates in nitrification, ammonium, and nitrite. If real, these core-top data suggest that nitrification thoroughly oxidizes the nitrogen regenerated from organic matter in these surface sediments. Below 2 cm, nitrate diffuses downward and is reduced or consumed until its concentration approaches zero at about 10 cm. Ammonium concentrations are somewhat scattered, but suggest a peak between the most intense zones of nitrification and denitrification, followed by a greater increase below 12 cm where a small amount of SO_4^{2-} reduction may be occurring. The ammonium peak near the depth corresponding to the inflection point of the nitrate profiles indicates that organic nitrogen released during early stages of denitrification or MnO_2 reduction may not always be oxidized to nitrogen gas as was assumed by Emerson et al. (1980).

Values of interstitial water Mn^{2+} and Fe^{2+} (Fig. 3) resemble profiles reported by Emerson et al. (1980) from MANOP site M (water depth = 3,100 m), and by Sawlan and Murray (1983) from the Mexican continental shelf. These three sets of Mn^{2+} profiles "turn over" below one or two middepth peaks. It would be difficult to predict a zero oxygen boundary from the Mn^{2+} profiles in Fig. 3. Low levels of Fe^{2+} appear to be diffusing into the denitrification zone, especially in the FVGR core. The brown-green color change attributed by Lyle (1983) to the reduction of Fe^{3+} to Fe^{2+} was about 6 cm deep in these cores.

Silicate concentrations in the porewaters are not direct indicators of respiration reactions, but may reflect historical fluctuations in the rain rate of biogenic components to the sea floor. At the Patton Escarpment site silicate increases exponentially to 350–360 μmol kg^{-1} and then decreases. We do not know whether this trend is the result of a change in the silica accu-

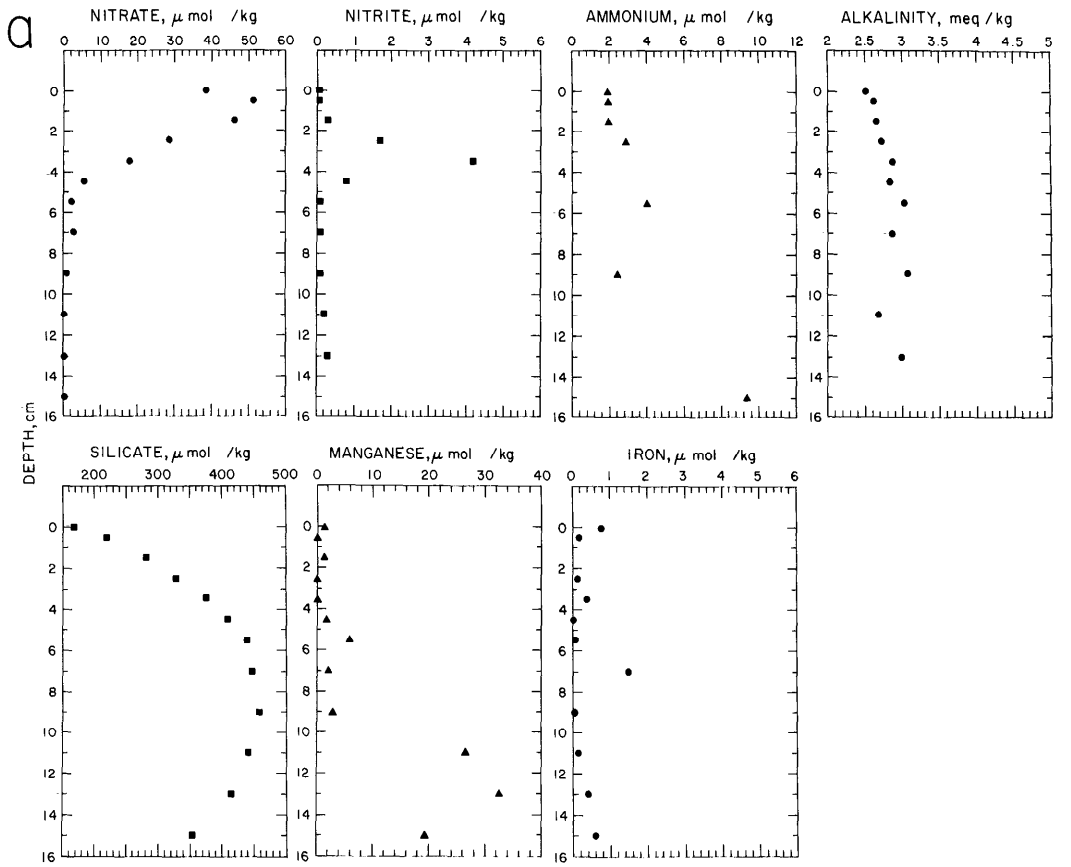

Fig. 3. Porewater results from the box core (a) and FVGR Sta. 124 grabs (b). Because two subcores were sectioned for each set of profiles, the porewaters from one subcore were divided to determine ammonium and alkalinity, whereas the porewaters from the remaining subcore were analyzed for nitrate, nitrite, manganese, iron, and silicate. All data points at 0 cm represent analyses of water overlying the cores.

mulation rate or of uptake reactions in the underlying sediments. However, the increasing carbonate carbon concentrations in Fig. 2 indicate that sedimentation in the area of the Patton Escarpment has varied during the time represented by 18 cm of sediment (~30,000 years: Gieskes et al. 1981).

Stoichiometry—The trends in the porewater data in Fig. 3 contain information about the stoichiometry of organic matter oxidation reactions as well as spatial relationships of reaction zones. Oxic respiration and nitrification reactions have frequently been assumed to occur concurrently in marine sediments, producing 124 CO_2 molecules and 16 NO_3^- molecules for every 138 O_2 consumed (Emerson et al. 1980; Jahnke et al. 1982). This stoichiometry is based on the additional hypothesis that the organic matter that is degraded has Redfield C:N ratios. Oxygen:nitrate stoichiometric ratios must be further corrected for the relative diffusivities of oxygen and nitrate when downcore variations in ΔO_2 and ΔNO_3^- are compared and have proven to be correct only within wide margins (Grundmanis and Murray 1982; Jahnke et al. 1982; Reimers et al. 1984).

The nitrate concentrations in the box and FVGR cores rose by 18.0 and 22.1 μmol kg^{-1} above the mean nitrate concentration determined from the bottom water samples taken initially by the FVGR syringe samplers (33.3 μmol kg^{-1}). The value predicted by the Redfield model is ~19 if bottom

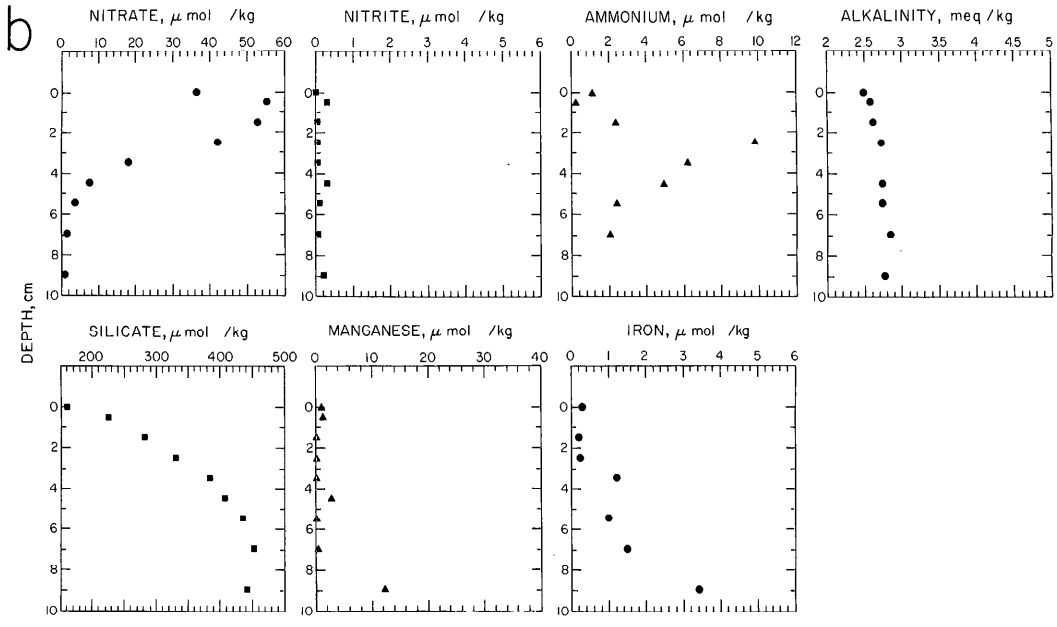

Fig. 3. Continued.

water oxygen equals 135.9 μmol kg^{-1} and nitrification goes to completion. This surprisingly good agreement suggests that past studies may have been limited more by problems in sampling the sediment–water interface than by problems with the nitrate model (Bender and Heggie 1984). It also is consistent with the small exchange of ammonium measured (Table 2) and supports the assumption made above that nitrification kinetics are sufficiently rapid to consume a major fraction of the regenerated nitrogen before it can exchange across the sediment–water interface of this site. The nitrate gradients cannot be reconciled with the small nitrate fluxes actually measured and reported in Table 2, however. Nitrate fluxes measured at the Patton Escarpment previously (0.017±0.005 μmol cm^{-2} day^{-1}: Smith et al. 1983) are probably more representative of the true in situ nitrate flux.

The predicted vs. measured oxygen flux: A final analysis—The data which constrain a diffusion model prediction of the oxygen flux at the Patton Escarpment presented in Table 3 are used in Fig. 4 to compare a range of calculated fluxes to the FVGR measured fluxes. The shaded area in the figure represents the oxygen flux estimates for the site using the oxygen gradients and porosity determinations at distances between 0 and 0.3 cm relative to the sediment–water interface. These estimates predict oxygen consumption rates between 0.14 and 0.22 μmol cm^{-2} d^{-1}, and they are *best* estimates because they incorporate data collected as near as possible to the interface.

If we extrapolate linear oxygen gradients over greater depths (i.e. move to the left along the horizontal axis in Fig. 4), or if we limit the sediment diffusion coefficient to a specific value, the size of the shaded area increases or decreases accordingly. On the assumption that the measured in situ fluxes are in fact representative of an undisturbed, nonenclosed seafloor, this scheme is a useful technique for identifying the correct parameters for determining calculated fluxes across the sediment–water interface. For example, it is obvious from Fig. 4 that if our microelectrode oxygen gradients are not over- or underestimated, the best overlap between the measured and predicted oxygen exchange rates occurs if the bulk sediment dif-

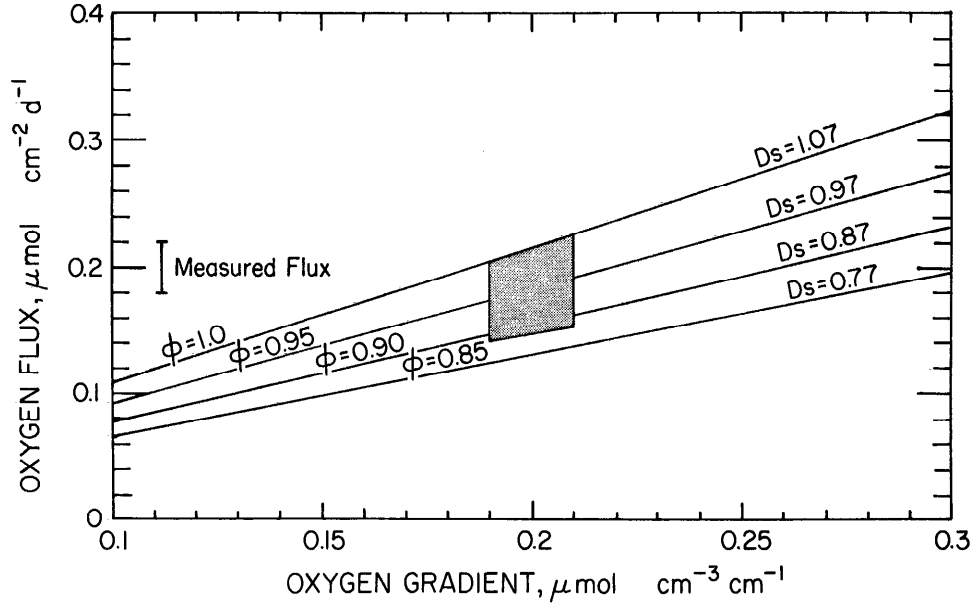

Fig. 4. Benthic oxygen flux vs. the oxygen gradient at the sediment–water interface. The different lines represent the linear relationships predicted by Fick's law of diffusion with different boundary conditions limiting the parameters ϕ and D_s. The shaded area indicates the range of fluxes derived from the data collected as near as possible to the sediment–water interface in this study.

fusion coefficient D_s is between 90 and 100% of the value of the molecular diffusion coefficient, D_o. This result is in agreement with findings from studies of the uptake rate of the conservative tracer $^{22}Na^+$ by sediments enclosed by the chambers of the MANOP Lander (Jahnke et al. 1983). It is further reconciled if we keep in mind that there is likely to be a >10% error in D_o (Broecker and Peng 1974).

Thus, the comparison made in Fig. 4 is inspired by a picture of the deep sea floor in which the mechanisms controlling oxygen fluxes and organic matter degradation are simple but apparently realistic. A more detailed interpretation of all the data presented expands the picture so that at any given time a large portion of the particulate organic matter reaching the sediment–water interface is viewed as being oxidized rapidly (order, days to months) within the upper few millimeters of the sediment column. These reactions then limit the rate at which molecular oxygen is supplied by diffusion across the sediment–water interface, which in turn balances the rate of total sediment community oxygen consumption. As the seasonal supply of particulate carbon increases or decreases, the oxygen demand in the upper sediment also varies, and the gradients must steepen and relax. Nondiffusive exchange processes such as irrigation through burrows and tubes are relatively unimportant for determining oxygen fluxes. Organisms that move over the sediment–water interface must disturb the system, but because the time required to re-establish diffusive exchange to a few millimeters depth is of the order of a few hours, very high rates of activity appear to be necessary to greatly enhance diffusive fluxes of oxygen. Indirectly, macrofaunal activities may lead to faster reaction kinetics, i.e. to more rapid microbial degradation of organic matter (Aller 1978; Reimers and Suess 1983), but this would not be reflected in differences between measured and predicted fluxes.

The major problem with the above proposal is that we have adjusted the parameters for predicting oxygen fluxes in order to match the measured rates and then we have concluded that the most probable transport mechanism is indeed diffusion. There may be errors in measuring in situ

exchange rates of oxygen (Smith 1978; Smith and Hinga 1983; Reimers and Suess 1983) or oxygen profiles in decompressed cores (Reimers et al. 1984) that bias or invalidate our conclusions. The worst possible case would be if enclosure of a volume of sediment and overlying water in a grab on the sea floor inhibits natural nondiffusive exchange processes and artificially establishes the diffusion regime we have described. The only evidence that this is not the case comes from the studies mentioned previously which document other mechanisms of nutrient and tracer exchange in shallow water marine environments (Klump and Martens 1981; McCaffrey et al. 1980). These studies were similar in experimental design to our study, but they confirmed that biological transport processes can enhance benthic fluxes by as much as a factor of four over those supported by vertical molecular diffusion. This was especially true for nutrients that diffuse from production zones located well below the sediment–water interface. Thus, although biological exchange processes can be detected by current methods, they apparently are directly responsible for only a small portion of the total benthic oxygen flux at our deep water site. Although more comparisons are needed, we conclude that it is valid to assume that simple diffusion of oxygen from overlying waters is the dominant deep sea pathway fueling sediment community oxygen consumption and that most of this oxidation occurs within a few millimeters of the sediment–water interface.

References

ALLER, R. C. 1978. Experimental studies of changes produced by deposit feeders on porewater, sediment, and overlying water chemistry. Am. J. Sci. **278:** 1185–1234.

———. 1980. Quantifying solute distributions in the bioturbated zone of marine sediments by defining an average microenvironment. Geochim. Cosmochim. Acta **44:** 1955–1966.

———. 1984. The importance of relict burrow structures and burrow irrigation in controlling sediment solute distributions. Geochim. Cosmochim. Acta **48:** 1929–1934.

ANDREWS, D., AND B. T. HARGRAVE. 1984. Close interval sampling of interstitial silicate and porosity in marine sediments. Geochim. Cosmochim. Acta **48:** 711–722.

BENDER, M. L., AND D. T. HEGGIE. 1984. Fate of organic carbon reaching the deep sea floor: A status report. Geochim. Cosmochim. Acta **48:** 977–986.

BERNER, R. A. 1980. Early diagenesis: A theoretical approach. Princeton.

BOUDREAU, B. P., AND N. L. GUINASSO, JR. 1982. The influence of a diffusive sublayer on accretion, dissolution, and diagenesis at the sea floor, p. 115–146. *In* K. A. Fanning and F. T. Manheim [eds.], The dynamic environment of the ocean floor. Lexington.

BROECKER, W. S., AND T.-H. PENG. 1974. Gas exchange rates between air and sea. Tellus **26:** 21–35.

DEFLAUN, M. F., AND L. M. MAYER. 1983. Relationships between bacteria and grain surfaces in intertidal sediments. Limnol. Oceanogr. **28:** 873–881.

EMERSON, S. R., K. FISCHER, C. REIMERS, AND D. HEGGIE. 1985. Organic carbon dynamics and preservation in deep sea sediments. Deep-Sea Res. **32:** 1–21.

———, AND OTHERS. 1980. Early diagenesis in sediments from the eastern equatorial Pacific. 1. Pore water nutrient and carbonate results. Earth Planet. Sci. Lett. **49:** 57–80.

FROELICH, P. N., AND OTHERS. 1979. Early oxidation of organic matter in pelagic sediments of the eastern equatorial Atlantic: Suboxic diagenesis. Geochim. Cosmochim. Acta **43:** 1075–1090.

GIESKES, J., B. NEVSKY, AND A. CHAIN. 1981. Interstitial water studies, Leg 63. Init. Rep. Deep-Sea Drilling Proj. **63:** 623–629.

———, AND W. C. ROGERS. 1973. Alkalinity determination in interstitial waters of marine sediments. J. Sediment. Petrol. **43:** 272–277.

GOLOWAY, F., AND M. BENDER. 1982. Diagenetic models of interstitial nitrate profiles in deep sea suboxic sediments. Limnol. Oceanogr. **27:** 624–638.

GRUNDMANIS, V., AND J. W. MURRAY. 1982. Aerobic respiration in pelagic marine sediments. Geochim. Cosmochim. Acta **46:** 1101–1120.

HINGA, K. R., J. MCN. SIEBURTH, AND G. R. HEATH. 1979. The supply and use of organic material by the deep-sea benthos. J. Mar. Res. **37:** 557–579.

JAHNKE, R. A., D. HEGGIE, S. EMERSON, AND V. GRUNDMANIS. 1982. Pore waters of the central Pacific Ocean: Nutrient results. Earth Planet. Sci. Lett. **61:** 233–256.

———, AND OTHERS. 1983. The bottom lander. Eos **64:** 721.

KLUMP, J. V., AND C. S. MARTENS. 1981. Biogeochemical cycling in an organic rich coastal marine basin—2. Nutrient sediment-water exchange processes. Geochim. Cosmochim. Acta **45:** 101–122.

LYLE, M. 1983. The brown-green color transition in marine sediments: A marker of the Fe (III)-Fe(II) redox boundary. Limnol. Oceanogr. **28:** 1026–1033.

MCCAFFREY, R. J., AND OTHERS. 1980. The relationship between pore water chemistry and benthic fluxes of nutrients and manganese in Narragansett Bay, Rhode Island. Limnol. Oceanogr. **25:** 31–44.

MARTENS, C. S., AND J. V. KLUMP. 1980. Biogeochemical cycling in Cape Lookout Bight—1. Methane sediment-water exchange processes. Geochim. Cosmochim. Acta **44:** 471–490.

MULLIN, J. B., AND J. P. RILEY. 1955. The colorimetric determination of silicate with special reference to sea and natural waters. Anal. Chim. Acta **12:** 162–176.

MURRAY, J. W., AND V. GRUNDMANIS. 1980. Oxygen consumption in pelagic marine sediments. Science **209:** 1527–1530.

PORTER, K. G., AND Y. S. FEIG. 1980. The use of DAPI for identifying and counting aquatic microflora. Limnol. Oceanogr. **25:** 943–948.

REIMERS, C. E., S. KALHORN, S. R. EMERSON, AND K. H. NEALSON. 1984. Oxygen consumption rates in pelagic sediments from the Central Pacific: First estimates from microelectrode profiles. Geochim. Cosmochim. Acta **48:** 903–911.

———, AND E. SUESS. 1983. The partitioning of organic carbon fluxes and sedimentary organic matter decomposition rates in the oceans. Mar. Chem. **13:** 141–168.

SAWLAN, J. J., AND J. W. MURRAY. 1983. Trace metal remobilization in the interstitial waters of red clay and hemipelagic marine sediments. Earth Planet. Sci. Lett. **64:** 213–230.

SAYLES, F. L. 1979. The composition and diagenesis of interstitial solutions, 1. Fluxes across the sediment-water interface in the Atlantic Ocean. Geochim. Cosmochim. Acta **43:** 527–546.

SMITH, K. L., JR. 1978. Benthic community respiration in the N.W. Atlantic Ocean: In situ measurements from 40 to 5200 m. Mar. Biol. **47:** 337–347.

———, AND R. J. BALDWIN. 1983. Deep-sea respirometry: In situ techniques, p. 298–319. *In* H. Forstner and E. Gnaiger [eds.], Polarographic oxygen sensors: Aquatic and physiological applications. Springer.

———, AND ———. 1984. Seasonal fluctuations in deep-sea sediment community oxygen consumption: Central and eastern North Pacific. Nature **307:** 624–626.

———, AND K. R. HINGA. 1983. Sediment community respiration in the deep sea, p. 331–370. *In* G. T. Rowe [ed.], The sea, v. 8. Wiley.

———, M. LAVER, AND N. BROWN. 1983. Sediment community oxygen consumption and nutrient exchange in the central and eastern North Pacific. Limnol. Oceanogr. **28:** 882–898.

———, G. A. WHITE, AND M. B. LAVER. 1979. Oxygen uptake and nutrient exchange of sediments measured in situ using a free vehicle grab respirometer. Deep-Sea Res. **26:** 337–346.

———, ———, ———, AND J. A. HAUGSNESS. 1978. Nutrient exchange and oxygen consumption by deep-sea benthic communities: Preliminary in situ measurements. Limnol. Oceanogr. **23:** 997–1005.

SNIDER, L. J., B. R. BURNETT, AND R. R. HESSLER. 1984. The composition and distribution of meiofauna in a central North Pacific deep-sea area. Deep-Sea Res. **31:** 1225–1249.

STRICKLAND, J. D., AND T. R. PARSONS. 1972. A practical handbook of seawater analysis, 2nd ed. Bull. Fish. Res. Bd. Can. 167.

ULLMAN, W. J., AND R. C. ALLER. 1982. Diffusion coefficients in nearshore marine sediments. Limnol. Oceanogr. **27:** 552–556.

YAYANOS, A. A., AND A. S. DIETZ. 1982. Thermal inactivation of a deep-sea bacterium, isolate CNPT-3. Appl. Environ. Microbiol. **43:** 1481–1489.

Submitted: 25 September 1984
Accepted: 12 September 1985